

Design of Nonsteroidal Anti-Inflammatory Drug-Based Ionic Liquids with Improved Water Solubility and Drug Delivery

Guillaume Chantereau,^{†,‡} Mukesh Sharma,^{†,‡} Atiye Abednejad,[†] Bruno M. Neves,[§] Gilles Sèbe,[‡] Véronique Coma,[‡] Mara G. Freire,^{*,†,‡} Carmen S. R. Freire,^{†,‡} and Armando J. D. Silvestre^{*,†,‡}

[†]CICECO – Aveiro Institute of Materials, Department of Chemistry, University of Aveiro, 3810-193 Aveiro, Portugal

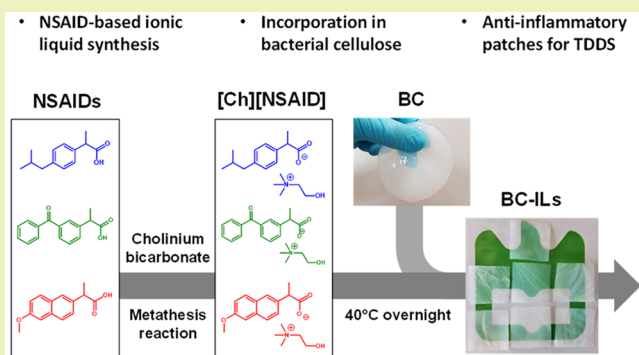
[‡]Laboratoire de Chimie des Polymères Organiques, University of Bordeaux, 16 Avenue Pey-Berlan, 33607 Pessac Cedex, France

[§]Department of Medical Sciences and Institute of Biomedicine – iBiMED, University of Aveiro, 3810-193 Aveiro, Portugal

Supporting Information

ABSTRACT: We here report the synthesis of ionic liquids (ILs) composed of the cholinium cation and anions derived from nonsteroidal anti-inflammatory drugs (NSAIDs), namely ibuprofen, ketoprofen, and (S)-naproxen, and their incorporation into bacterial nanocellulose envisaging their use in topical drug delivery systems. The chemical structure of the synthesized ILs was confirmed by spectroscopic techniques, and thermal analysis confirming their categorization as ionic liquids with melting temperatures below 100 °C and resistance to autoclaving. The synthesized ILs display an aqueous solubility (at pH 7.4) ranging between 120 and 360 mM, which is up to 100 times higher than the solubility of the respective NSAID precursors, thus contributing to improved bioavailability. Their incorporation into bacterial cellulose originated transparent and homogeneous membranes. Thermogravimetric analysis (stable up to at least 225 °C) and mechanical assays (with minimum Young's modulus of 937 MPa, maximum stress of 33 MPa and elongation at break of 5.6%) confirmed the suitability of the prepared membranes for application as topical drug delivery systems. Furthermore, the rehydration ability of IL-incorporated membranes is 18 to 26 times higher than bacterial cellulose, being valuable to the absorption of exudates. Release tests demonstrated a faster and complete release of the IL-based drugs when compared with the starting NSAIDs. Finally, it is demonstrated that bacterial cellulose is not cytotoxic nor proinflammatory, whereas the cytotoxicity and anti-inflammatory properties of IL-incorporated BC membranes are similar to those of NSAIDs or ILs, reinforcing their suitability as envisioned materials for topical drug release applications.

KEYWORDS: Nonsteroidal anti-inflammatory drugs, Ionic liquids, Cholinium cation, Bacterial nanocellulose, Topical drug delivery



INTRODUCTION

Nonsteroidal anti-inflammatory drugs (NSAIDs) are the most commonly used pharmaceutical ingredients for inflammation relief.¹ Their main action is through the inhibition of cyclooxygenases, minimizing the production of prostaglandins, responsible for pain and inflammation responses.² However, most NSAIDs are poorly water-soluble,³ which is a major drawback when envisaging their incorporation into hydrophilic matrices for drug release and bioavailability.

The low water solubility of NSAIDs, and in of particular ibuprofen, ketoprofen, and (S)-naproxen (0.07–0.20 mM), can be overcome calling upon various approaches.⁴ The use of the respective salt forms is the simplest strategy. For example, sodium ibuprofen, sodium naproxen, and sodium diclofenac reach water solubilities of about 10² mM, with the exception of sodium ketoprofen that is considerably less soluble (0.06 mM).⁴ Koç et al.⁵ enhanced ibuprofen and ketoprofen water solubility up to 10¹ mM by their encapsulation in poly-

(propylene oxide)/polyamidoamine-based dendrimers. The preparation of nanosuspensions of ibuprofen with improved dissolution rate and lower gastric irritancy has also been described.⁶

More recently, ionic liquids (ILs) comprising active pharmaceutical ingredients (APIs) have been developed to improve the water solubility of different drugs. This strategy is similar to the preparation of more common drug salt forms, yet combining large organic ions, leading to lower melting temperatures.⁷ ILs in particular have raised interest due to their negligible vapor pressure, high thermal stability, and low flammability.⁸ Cholinium-based ILs were designed for the first time in 1962 with the salicylate counterion, resulting in improved water solubility in comparison to salicylic acid, while

Received: May 17, 2019

Revised: July 10, 2019

Published: July 17, 2019

preserving the respective anti-inflammatory properties.⁹ Subsequent studies have been performed with cholinium-based ILs comprising APIs for improved water solubility, such as cholinium-nalidixate,¹⁰ cholinium-sulfasalazine,¹¹ and cholinium-ampicillin.⁸ Recently, Santos et al.¹² reported on the synthesis of ibuprofen-based ILs, yet combined with different organic cations, such as 4 quaternary ammonium derivatives including cholinium, 4 imidazolium derivatives, and cetylpyridinium. However, the cholinium-ibuprofen organic salt they designed had a melting temperature of 104 °C and thus do not fit in the ionic liquids category.

The oral administration of NSAIDs is currently the most used route.¹³ However, this type of administration presents several drawbacks, such as possible side effects in the gastrointestinal tract¹⁴ and liver damage.² Therefore, whenever possible, topical administration of anti-inflammatory drugs is the most efficient way to reduce most of these side effects.¹⁵ Topical delivery can be achieved with creams, gels, and patches. Creams and gels are simple to use but lack in control of the applied dose and skin surface covered. Patches are generally composed of three components: a drug-containing matrix (e.g., acrylic-acid polymers, cellulose derivatives, silicone, among others), an outer membrane (e.g., poly(vinyl alcohol), polyurethane, among others), and a rate controlling layer (e.g., poly(ethylenevinylacetate), polyethylene, poly(4-methyl-1-pentene), among others).^{16,17} First used patches were additionally composed of an adhesive layer; whereas in novel products tend to favor matrices with inherent adhesiveness. Recently, novel drug-incorporating patches composed of a single layer have been proposed. For instance, Tombs et al.¹⁸ produced patches made of a single poly(ether-urethane)-silicone membrane containing ibuprofen. However, the future of topical patches resides in the materials beneficial properties that ideally should permit the use of single layer structures and green processing and be of a biobased and biodegradable nature.

Cellulose produced by bacteria, known as bacterial nanocellulose (BC), is synthesized by several nonpathogenic bacteria of the genus *Gluconacetobacter*, *Sarcina*, or *Agrobacterium*.¹⁹ BC has raised considerable interest in the pharmaceutical field because of its unique properties, namely a nanofibrillar structure, high water-holding capacity, moldability, and good mechanical properties.¹⁹ BC membranes are able to promote a controlled release of drugs, being explored by different research groups to develop topical drug delivery systems (TDDS) for different drugs or biologically active molecules, e.g. S-propranolol,²⁰ benzalkonium chloride,²¹ sodium diclofenac,²² and caffeine.²³ However, in the case of low water-soluble APIs, such as ibuprofen, organic solvents are required to guarantee its incorporation in the BC membranes.²⁴

In this context, the aim of this work was to synthesize and characterize NSAID-based ionic liquids, namely cholinium ibuprofenate, cholinium ketoprofenate, and cholinium naproxenate, aiming at improving the water solubility of these drugs and incorporate them into BC membranes to develop effective TDDS. Briefly, NSAID-based ILs were synthesized and characterized by ¹H and ¹³C NMR, FTIR, TGA, and DSC. Furthermore, their solubility in PBS aqueous solutions at 25 °C was determined, as well as their cytotoxicity and anti-inflammatory properties. For comparison purposes, these characterizations were also performed on the NSAIDs precursor drugs. ILs and NSAIDs were incorporated into BC

membranes and characterized in terms of thermal and mechanical properties. The release of the ILs and original NSAIDs from the BC membranes was then investigated. Finally, the cytotoxicity and anti-inflammatory properties of the IL-loaded membranes were determined to confirm their potential for topical drug delivery applications.

EXPERIMENTAL SECTION

Materials. Cholinium bicarbonate, 80% in water, racemic ibuprofen ≥98% (Ibu), Dulbecco's Modification of Eagle's Medium (DMEM) c and fetal bovine serum (FBS) were purchased from Sigma-Aldrich, USA. Racemic ketoprofen 98% (Ket) and (S)-naproxen 99% (Nap) were supplied by Alfa Aesar, Germany. Raw 264.7 macrophages (TIB-71) were acquired from American Type Culture Collection, Manassas, USA. All chemicals were used as received.

Synthesis of NSAID-Based Ionic Liquids. NSAID-based ionic liquids (ILs) ([Ch][NSAID]), namely cholinium ibuprofenate ([Ch][Ibu]), cholinium ketoprofenate ([Ch][Ket]), and cholinium naproxenate ([Ch][Nap]), were synthesized by simple metathesis reactions as reported in detail elsewhere.²⁷ Briefly, a 1:1.05 molar ratio of cholinium bicarbonate and each NSAID were mixed, by the addition of 11.50, 12.93, and 11.71 g of ibuprofen, ketoprofen, and (S)-naproxen, respectively, into 10 g of cholinium bicarbonate, 80% in water. Synthesized ILs were washed three times with ethyl acetate to remove unreacted NSAIDs. Excess solvent and water were removed under reduced pressure using a rotary evaporator (60 °C, 30 min) and a nitrogen vacuum line (60 °C, 72 h, ca. 0.01 mbar). Dried ILs were finally collected (water content below 2.12 wt %; determined by Karl Fischer Titration (Metrohm 831 Karl Fisher coulometer); see the [Supporting Information](#)) and stored in closed vials at 4 °C up to characterization and use. The optical rotation of [Ch][Nap] was measured using a polarimeter JASCO P-2000 at 589 nm, demonstrating that its specific rotation was $-9.6 \pm 0.3^\circ$.

Bacterial Cellulose Production. BC membranes were prepared by growing the bacterial strain *Gluconacetobacter sacchari*²⁸ following a previously described protocol.²⁹ After 6 days of incubation, BC membranes were withdrawn from the culture medium and treated in alkaline conditions, at 90 °C, prior to washing with distilled water. This step was repeated until neutral pH was reached. Wet BC membranes were stored in distilled water at 4 °C until use.

Incorporation of NSAIDs and ILs into Bacterial Cellulose. Wet BC membranes were cut in 2 × 2 cm² rectangular pieces (99.33 ± 0.20% water content). For the incorporation of NSAIDs, BC membranes were submitted to a solvent exchange with ethanol (5 times 1 h soaking in ethanol), and then *circa* 50% of their ethanol content was drained. BC membranes were then soaked in 1 mL of ethanol solutions containing 10 mg·mL⁻¹ ibuprofen, ketoprofen, or (S)-naproxen, as controls. In the case of ILs, the solvent exchange step was not necessary due to their high water solubility. 2 × 2 cm² BC samples were pressed until *circa* 50% of their water content was drained. The concentration was adapted to obtain BC-IL membranes with 10 mg of NSAID, namely 15.0, 14.1, and 14.5 mg·mL⁻¹ for [Ch][Ibu], [Ch][Ket], and [Ch][Nap], respectively.

After complete absorption of the solutions, membranes were dried at 40 °C. Dried membranes were kept in a desiccator until use. After the recovery of the dried membranes, sample holders were rinsed with 4 mL of adequate solvent, and the content of IL or NSAID in the solvent was determined by UV-vis spectroscopy (see the [Supporting Information](#)).

For tensile tests, 7 × 7 cm² membranes were prepared with adapted NSAID- or IL-volumes of the solutions.

Characterization Techniques. ¹H and ¹³C NMR spectra of [Ch][NSAID] ILs were recorded on a Bruker Avance 300 at 300.13 and 75.47 MHz, respectively, using deuterated water (D₂O) as solvent. ¹³C solid-state cross-polarized magic-angle spinning nuclear magnetic resonance spectra of BC and BC-[Ch][NSAID] membranes were recorded on a Bruker Avance 400 spectrometer. Samples were packed into a zirconia rotor sealed with Kel-F caps and spun at 7 kHz.

The acquisition parameters were as follows: 4 μ s 90° pulse width, 2 ms contact time, and 4 s dead time delay.

The determination of NSAIDs and [Ch][NSAID] concentrations in ethanol and phosphate buffer solutions at pH 7.4 (PBS, 0.1 M) was carried out by UV–vis spectroscopy, using a Thermo Scientific Evolution 600 spectrophotometer. Selected maximum wavelengths in PBS were 221, 230, 259, 260, 230, and 230 nm for ibuprofen, [Ch][Ibu], ketoprofen, [Ch][Ket], (S)-naproxen, and [Ch][Nap], respectively. The wavelengths used for their quantification in ethanol were 218, 251, and 271 nm for ibuprofen, ketoprofen, and (S)-naproxen, respectively. An excess of each compound was added to the PBS or ethanol solution and allowed to equilibrate at 25 °C under 750 rpm for 72 h. After equilibration, solutions were centrifuged during 8 min at 8000 rpm. Supernatant was recovered and centrifuged again. Saturated aqueous solutions were diluted by successive 10-fold dilutions, and their concentration was determined by UV–vis spectroscopy as described. Experiments were carried out in duplicate, and the average value and corresponding standard deviation are given.

FTIR spectra of NSAIDs, [Ch][NSAID] ILs, and BC membranes were obtained on a PerkinElmer spectrometer equipped with a single horizontal Golden Gate ATR cell. 32 scans were acquired in the 4000–800 cm^{-1} range, with a resolution of 4 cm^{-1} . Spectra were obtained in triplicate and averaged.

Glass transition and melting temperatures of [Ch][NSAID] ILs were measured on a power compensation differential scanning calorimeter, PerkinElmer model Pyris Diamond DSC, using hermetically sealed aluminum crucibles with a constant flow of nitrogen (50 $\text{mL}\cdot\text{min}^{-1}$). Samples of about 15 mg were used in each experiment. Glass transitions (T_g) and melting temperatures (T_{melt}) were taken as onset temperatures.

The decomposition temperatures of NSAIDs, [Ch][NSAID], and BC membranes were determined by TGA conducted on a Shimadzu TGA 50 analyzer equipped with a platinum cell. Samples were heated at a constant rate of 10 $^{\circ}\text{C}\cdot\text{min}^{-1}$, from room temperature up to 800 $^{\circ}\text{C}$, under a nitrogen flow of 20 $\text{mL}\cdot\text{min}^{-1}$. Thermal decomposition temperatures (T_{dec}) were taken as the maximum of the derivative of TG curves, and initiation of the decomposition temperatures ($T_{5\%}$) was taken as onset temperatures. Residue at 800 $^{\circ}\text{C}$ was calculated in terms of weight percentage of the dried material.

The surface morphology of BC, BC-NSAID, and BC-[Ch]-[NSAID] membranes was assessed by SEM by cutting an adequate size membrane sample, while for cross-section images membranes were broken after immersion in liquid nitrogen. Samples were then covered with carbon and analyzed on a Hitachi SU-70 microscope at 4 kV and 10 mm focal distance.

Tensile assays of BC, BC-NSAID, and BC-[Ch][NSAID] membranes were performed using an Instron 5944 testing machine with Bluehill 3 software in tensile mode with a 1 kN load cell. Samples were strips of 70 \times 10 mm^2 , and the gauge length was 30 mm. At least 5 strips were tested for each sample. The corresponding stress–strain curves permitted to determine Young's modulus (slope at 0.05% elongation), maximum stress, and elongation at break. Experiments were carried out in quintuplicate, and the average value and corresponding standard deviation are presented.

Rehydration tests were conducted for BC, BC-NSAID, and BC-IL membranes. Membranes were weighed and soaked in individual containers with 200 mL of PBS (pH 7.4; 0.1 M) aqueous solutions at room temperature, for 24 h. Samples were regularly taken out, the excess of water was gently removed, and membranes were weighted and reimmersed again. The absorbed aqueous solution, in g per g of dried material, was calculated according to eq 1

$$\text{PBS Absorption} = \frac{w_{\text{wet}} - w_{\text{dry}}}{w_{\text{dry}}} \quad (1)$$

where w_{dry} and w_{wet} are the weight of dried and wet samples, respectively. Experiments were carried out in triplicate, and the average value and corresponding standard deviation are presented.

BC-NSAID and BC-[Ch][NSAID] membranes were placed in closed flasks, containing 200 mL of PBS, under magnetic stirring and

protected from light. The release of NSAIDs and ILs was then evaluated. At determined time intervals (during 24 h), 2 mL of solution was withdrawn, and the same volume of fresh buffer was added to maintain the volume constant. NSAID or IL content in each aliquot was determined by UV–vis spectroscopy as previously described. The IL or NSAID content at each time was plotted as a cumulated percentage release, determined according to eq 2

$$C_{\text{cumul}} = C_n + \sum_{k=0}^{n-1} \frac{2 \times C_k}{200} \quad (2)$$

where C_n is the IL or NSAID concentration at time n . The mass of NSAID or IL leaching out from the sample was calculated and divided by the initial mass incorporated to get the released ratio (wt %). Experiments were carried out in triplicate, and the average value and corresponding standard deviation are presented.

The effect of NSAIDs, [Ch][NSAID], BC-NSAID, and BC-[Ch][NSAID] on Raw 264.7 macrophage viability was assessed by the resazurin assay. Cells were seeded in 96-well plates and incubated during 12 h to allow attachment, being then exposed for 24 h to concentrations ranging from 1 μM to 4 mM. In experiments with membranes, cells were plated in 6-well plates and allowed to stabilize overnight, and then membranes containing equivalent amounts of NSAIDs or ILs samples were placed into contact with cell cultures. The detailed protocol used is given elsewhere.²⁷ Experiments were carried out in triplicate, and the average value and corresponding standard deviation are presented. To calculate the EC_{50} values, dose–response curves were fitted with the nonlinear least-squares method using a linear logistic model.

The potential anti-inflammatory activity of NSAIDs, [Ch][NSAID] ILs, BC, BC-NSAIDs, and BC-[Ch][NSAID] membranes was tested by analyzing their capacity to inhibit lipopolysaccharide (LPS)-induced nitric oxide (NO) and prostaglandin E_2 (PGE2) production in macrophages. NO production was evaluated according to a previously described method.²⁶ Cells were incubated with the culture medium (control), nontoxic concentrations of NSAIDs (ibuprofen: 250 μM ; ketoprofen: 1 mM; (S)-naproxen: 1 mM), equivalent concentrations of [Ch][Ibu], [Ch][Ket], [Ch][Nap], and with respective membrane-conditioned media for 24 h. PGE2 was quantified in cell supernatants using an ELISA kit according to the manufacturer's instructions (R&D Systems, Minneapolis, USA).

Multiple group comparisons were made by One-Way ANOVA analysis, with a Dunnett's Multiple Comparison post-test. Statistical analysis was performed using GraphPad Prism, version 6.01 (GraphPad Software, San Diego, CA, USA). Significance levels are as follows: * $p < 0.05$, ** $p < 0.01$, *** $p < 0.001$, **** $p < 0.0001$ for control vs treatment conditions; # $p < 0.05$, ## $p < 0.01$, ### $p < 0.001$, #### $p < 0.0001$ for LPS vs treatment conditions.

RESULTS AND DISCUSSION

Synthesis and Characterization of [Ch][NSAID] ILs. Cholinium-NSAID-based ionic liquids were synthesized by neutralization of cholinium bicarbonate with three anti-inflammatory acids, namely ibuprofen (Ibu), ketoprofen (Ket), and (S)-naproxen (Nap), resulting in cholinium ibuprofenate ([Ch][Ibu]), cholinium ketoprofenate ([Ch]-[Ket]), and cholinium naproxenate ([Ch][Nap]). The chemical structures of the NSAIDs and synthesized ILs are given in Figure 1.

The purity of the synthesized ILs was confirmed by ^1H and ^{13}C NMR. The respective spectra and cholinium:NSAID molar ratios, based on the ratio of the area of ammonium methyl groups' singlet of cholinium cation and the area of the αCH_3 proton doublets of NSAIDs, are given in the Supporting Information.

Fourier transformed infrared (FTIR) spectra of [Ch]-[NSAID] ILs, NSAIDs, and cholinium bicarbonate were

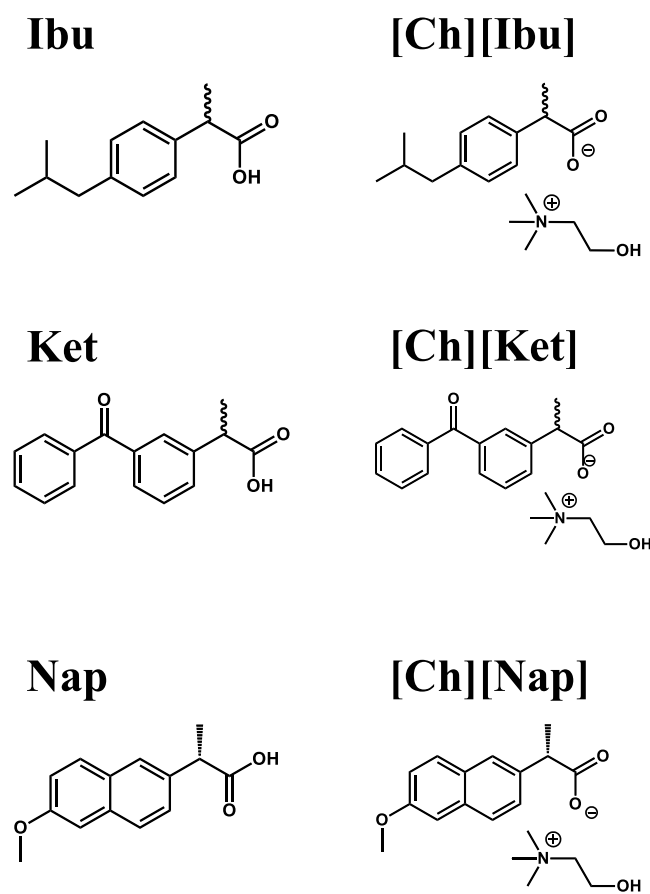


Figure 1. Chemical structures of NSAIDs and synthesized NSAID-based ILs.

recorded, and the corresponding spectra are given in the [Supporting Information](#). The successful synthesis of ILs was confirmed by the disappearance of the $\nu(\text{C}=\text{O})$ vibration of the acid group at 1709, 1690, 1721, and 1684 cm^{-1} for Ibu, Ket, non-hydrogen-bonded Nap, and hydrogen-bonded Nap, respectively.³⁰ On the other hand, the appearance of the $\nu_{\text{as}}(\text{C}=\text{O})$ band of the carboxylate group at 1565, 1570, and 1562 cm^{-1} is observed only for the non-IL forms, namely Ibu, Ket, and Nap. Moreover, the spectra of all ILs show the $\delta(\text{C}-\text{O})$ vibration of cholinium at 955 cm^{-1} .

Decomposition temperatures of the prepared [Ch][NSAID] ILs were assessed by thermogravimetric analysis (TGA), while glass transition and melting temperatures were determined by differential scanning calorimetry (DSC) and reported in [Table 1](#) (curves are given in the [Supporting Information](#)). The comparison of the [Ch][NSAID] decomposition temperatures (T_{dec}) with those of their NSAIDs precursors reveals a decrease of about 100 °C in the thermal stability, which is in accordance with literature data for other cholinium-based ILs.^{31–33} However, all ILs are at least stable up to 181 °C, which is enough to support sterilization procedures. Furthermore, [Ch][NSAID] ILs have glass transition temperatures (T_{g}) in the range from -90 to -70 °C. Their T_{g} values are however smaller than those of the NSAID precursors ([Table 1](#)). The same trend is observed for the ILs melting temperatures (T_{melt}), reaching values below 100 °C and fitting with the ILs general categorization.³⁴ This decrease in the melting temperatures is due to the introduction of an organic cation, resulting in ILs comprising ions of low charge density

Table 1. Thermal Properties of [Ch][NSAID] ILs and Respective NSAIDs^g

	T_{melt} (°C)	T_{g} (°C)	T_{dec} (°C)	solubility (mM)
Ibu	79 ^a	$-50/-35$ ^d	280 ^a	1.8 ± 0.2
Ket	97 ^b	-6 ^e	359 ^b	5.1 ± 0.3
Nap	158 ^c	36 ^f	287 ^c	4.8 ± 0.1
[Ch][Ibu]	-24	-89	181	309 ± 42
[Ch][Ket]	58	-72	198	357 ± 18
[Ch][Nap]	71	-73	182	121 ± 19

^aTita et al. 2010.³⁶ ^bTita et al. 2013.³⁷ ^cSovizi et al. 2010.³⁸ ^dDudognon et al. 2008.³⁹ ^eSailaja et al. 2013.⁴⁰ ^fAlleso et al. 2009.⁴¹ ^gSolubility of [Ch][NSAID] ILs and NSAIDs in PBS aqueous solutions (pH 7.4, 0.1 M).

and with poor coordination. Among the prepared ILs, [Ch][Ibu] has the lowest T_{melt} , being liquid at room temperature.

Envisioning the desired topical application and drug delivery of ILs, the solubility of [Ch][NSAID] ILs and NSAIDs was determined in PBS (pH 7.4, 0.1 M) aqueous solutions, similar to previous studies showing good skin permeation rates using cholinium-phenolate²⁶ and imidazolium-based²⁵ ILs. PBS was selected to mimic the cytoplasm of dermal cells and the extracellular medium.³⁵ The respective results are given in [Table 1](#). Overall, there is an increase of up to 2 orders of magnitude in the solubility of [Ch][Ibu], [Ch][Ket], and [Ch][Nap] in comparison with the original NSAIDs, which is a relevant advantage when envisioning these drugs improved bioavailability and incorporation into hydrophilic matrices for controlled and enhanced drug release.

Incorporation of NSAID-ILs in Nanocellulose Membranes: Characterization and Kinetics of Release. The obtained [Ch][NSAID] ILs and NSAIDs for comparison purposes were incorporated into bacterial cellulose membranes. The average mass of NSAID and [Ch][NSAID] incorporated in BC was evaluated by UV-vis (see the [Supporting Information](#)). Both NSAIDs and ILs were incorporated in high percentages, ranging from $93.0 \pm 5.8\%$ to $99.8 \pm 0.5\%$ of the initial amount poured on top of BC for Ket and [Ch][Ibu], respectively.

After incorporation of each NSAID and IL in the BC membranes, their macroscopic appearance was inferred ([Figure 2A](#)). From a macroscopic view, BC-NSAID surfaces are more heterogeneous than BC without APIs; the presence of agglomerates is particularly visible for BC-Nap, in agreement with the lower solubility of Nap is the less in PBS aqueous solutions ([Table 1](#)). On the other hand, all BC membranes comprising [Ch][NSAID] ILs are homogeneous and as transparent as the original BC.

SEM images were additionally taken to investigate the surface and cross-section morphologies of membranes ([Figure 2B and C](#)). Surface images show that both BC-NSAIDs and BC-[Ch][NSAID] membranes preserve the nanofibrillar structure of BC. However, agglomerates are observed in BC-NSAID membranes, especially with BC-Nap, as discussed before. Also confirmed by SEM images, there are no agglomerates in the BC-[Ch][NSAID] samples. The absence of agglomerates in these reveals the higher affinity of BC toward ILs. When analyzing the cross-section images, it is clear that all samples present the typical lamellar structure of BC.

The structural characterization of BC-[Ch][NSAID] membranes was also carried out by solid-state ¹³C NMR and FTIR,

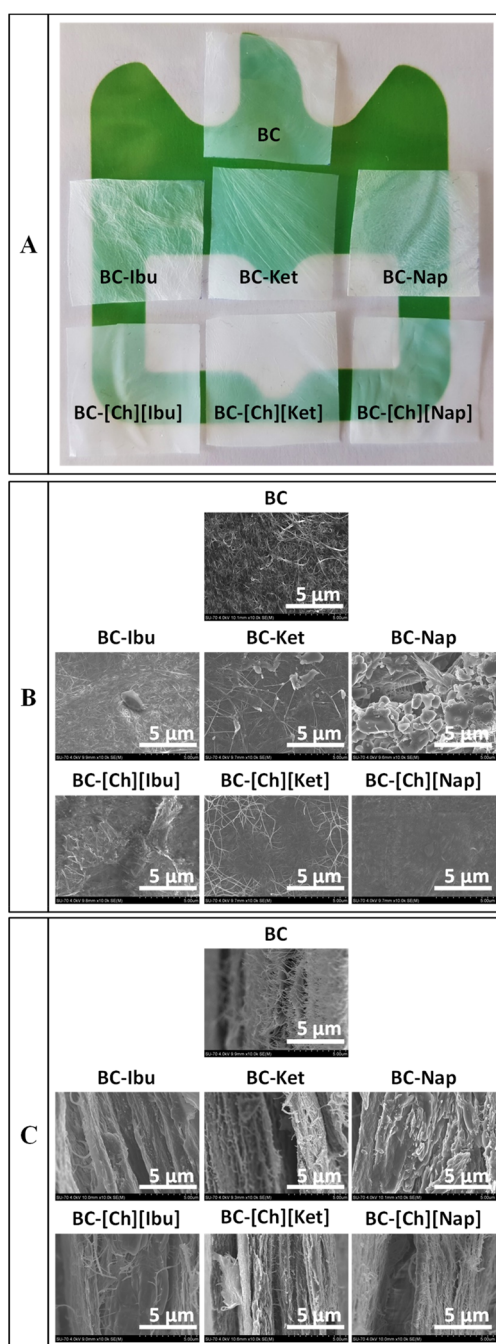


Figure 2. Macroscopic (A) and microscopic views by SEM of BC, BC-NSAID, and BC-IL surfaces (B) and cross sections (C) at a $\times 10k$ magnification.

whose results are given in the [Supporting Information](#). All membranes have typical resonances of BC at 65.3, 70.8–74.7, 88.9, and 106 ppm, assigned to BC6, BC2-BC3-BC5, BC4, and BC1 carbons, respectively. The [Ch][NSAID] resonance intensities are similar to those of BC, except for [Ch][Ket] whose resonances were smaller. Although no significant shift deviations are observed after the incorporation of [Ch][Ibu] and [Ch][Ket] into BC, stronger deviations are shown with [Ch][Nap], particularly in the peak corresponding to the methyl carbon C_{21} , from 18.2 to 13.9 ppm meaning that [Ch][Nap] establishes stronger interactions with BC. NMR observations are corroborated by FTIR analysis based on the presence of carboxylate stretching $\nu(C=O)$ in the 1570–1560

cm^{-1} region for BC-[Ch][Ibu] and BC-[Ch][Ket] and at 1548 cm^{-1} for BC-[Ch][Nap], thus confirming stronger interactions for the last IL-BC pair.

The thermal stability and decomposition profiles of BC-NSAID and BC-[Ch][NSAID] membranes were assessed by thermogravimetric analysis (TGA). The TGA curves of BC, BC-NSAIDs, and BC-[Ch][NSAID] and the corresponding derivative curves are given in the [Supporting Information](#). BC has the typical profile of cellulose with a first weight loss at 100 $^{\circ}C$, which is due to water evaporation, and a second weight loss at 338 $^{\circ}C$ due to cellulose decomposition. BC-NSAID samples show a thermal decomposition profile similar to that of BC, with T_{dec} in the range from 300 to 347 $^{\circ}C$ and $T_{5\%}$ in the range of 164–230 $^{\circ}C$. Only one decomposition step is seen since the studied NSAIDs have a maximum decomposition temperature similar to cellulose, ca. 300 $^{\circ}C$ ([Table 1](#)). The behavior of BC-[Ch][NSAID] samples is however different: a more significant first weight loss of 8.1–11.8 (wt %) due to water evaporation occurs, being in line with the higher ILs water affinity. Then, we observed a first weight loss which corresponds to the IL decomposition with a T_{dec} in the range of 225–254 $^{\circ}C$ and a $T_{5\%}$ in the range of 199–211 $^{\circ}C$ and a second weight loss corresponding to cellulose decomposition with a T_{dec} in the range of 307–322 $^{\circ}C$. Although a lower thermal stability is observed, BC-[Ch][NSAID] membranes are still able to support thermal treatments, such as autoclaving, required for sterilization prior to any healthcare or cosmetic application.

Mechanical properties of BC, BC-NSAID, and BC-IL membranes were investigated by tensile assays. Young's modulus, maximum stress, and elongation at break of different membranes, determined from the stress–strain curves, are given in the [Supporting Information](#). BC shows the characteristics of brittle elastic materials with high Young modulus (11842 ± 1239 MPa), high maximum stress (153 ± 46 MPa), and low elongation at break ($1.7 \pm 0.6\%$). The incorporation of NSAIDs in BC leads however to a strong decrease of the Young's modulus, down to 213 ± 15 , 3619 ± 1265 , and 117 ± 60 MPa for BC-Ibu, BC-Ket, and BC-Nap, respectively. A significant loss of maximum stress, viz. 38 ± 6 , 81 ± 23 , and 10 ± 3 MPa for BC-Ibu, BC-Ket, and BC-Nap, respectively, was also observed. On the other hand, when compared with pristine BC, elongation at break increases after incorporation of NSAIDs, up to 20.7 ± 1.7 , 2.9 ± 0.8 , and $12.7 \pm 2.7\%$ for BC-Ibu, BC-Ket, and BC-Nap, respectively. Nevertheless, a change in behavior from the elastic in BC to viscoplastic in BC-Ibu was observed, supporting the increase of elongation at break results, and which could be due to a plasticizing effect of ibuprofen. The incorporation of ILs into BC membranes leads to similar effects on their mechanical properties, namely to a decrease of the Young's modulus down to 720 ± 105 , 937 ± 343 , and 1191 ± 266 MPa, a decrease of maximum stress down to 33 ± 7 , 33 ± 7 , and 49 ± 17 MPa, and an increase in elongation at break up to 7.5 ± 3.4 , 8.4 ± 2.6 , and $5.7 \pm 3.2\%$ for BC-[Ch][Ibu], BC-[Ch][Ket], and BC-[Ch][Nap], respectively. These results can be compared with those obtained by Silva et al.⁴² who used bacterial cellulose films incorporating 5% of glycerol with 50 MPa maximum stress and 6.7% elongation at break. In summary, BC-[Ch][NSAID] membranes have significant maximum stress and elongation at break without the need of an additional compound to act as plasticizer.

The rehydration ability of membranes is an important parameter in what concerns the release of the target active compounds and membrane ability to absorb exudates. The results presented in Figure 3 (left), given in g of PBS aqueous

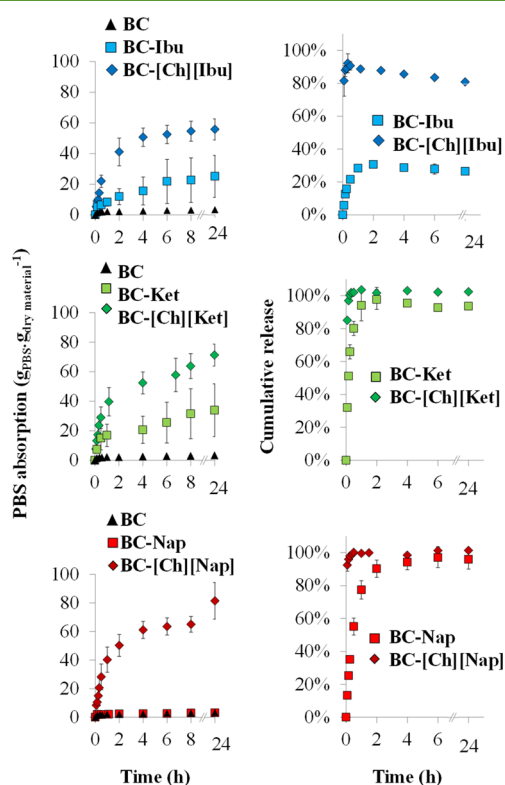


Figure 3. Rehydration experiment results in PBS (pH 7.4, 0.1 M) aqueous solutions for BC, BC-NSAID, and BC-[Ch][NSAID] membranes (left); cumulative release of NSAIDs and [Ch][NSAID] ILs in PBS aqueous solutions (right).

solution absorption *per g* of dried material, show a significantly higher PBS aqueous solution absorption capacity for the BC-Ibu and BC-Ket membranes after 24 h (25.1 ± 13.7 and 33.9 ± 18.0 , respectively), when compared with BC (3.3 ± 0.1), whereas BC-Nap does not show a significant increase of water absorption (3.1 ± 0.7). The low rehydration ability of BC-Nap samples can be attributed to the presence of Nap agglomerates in the BC surface as shown in Figure 2. The better dispersion of ibuprofen and ketoprofen in BC is important to reduce the collapsing of the BC structure during the drying process, thus improving the rehydration ability.⁴³ Furthermore, all BC-[Ch][NSAID] membranes have further improved PBS absorption ability when compared to the BC-NSAID references, with 55.7 ± 6.9 , 71.3 ± 7.4 , and 81.5 ± 12.7 for BC-[Ch][Ibu], BC-[Ch][Ket], and BC-[Ch][Nap], respectively, which is a remarkable advantage when considering the release of the target active compounds and membranes ability to absorb exudates. In comparison, Donnelly et al.,⁴⁴ using PEG-based hydrogels loaded with ibuprofen and ovalbumin, prepared patches for TDDS absorbing 18 g of PBS per g of dry material, while Lee et al. designed carboxymethylcellulose patches absorbing 5 g of water per g of dry material. This shows the extremely high rehydration capacity of our BC-ILs membranes.

The kinetics of release of NSAIDs and [Ch][NSAID] ILs from membranes in PBS aqueous solutions was investigated by

dissolution assays (Figure 3, right). The release of NSAIDs and [Ch][NSAIDs] follows the Weibull Model of first-order kinetics, meaning that BC does not show barrier properties in the diffusion of incorporated compounds. Parameters of the model and linear regression factors are given in the Supporting Information. All samples reached at least 90% of release after 2 h in 200 mL of PBS aqueous solution, except for BC-Ibu where only a 25.6% maximum release of Ibu was obtained. Ibuprofen is the most hydrophobic NSAID studied, as confirmed by its low solubility and its popularity in the literature.^{5,6} This value is also confirmed by Adeyeye et al.⁴⁵ who realized dissolution assays of ibuprofen in simulated intestine fluids and reached about 30% release, while topical patches containing ketoprofen⁴⁶ and naproxen⁴⁷ exhibited complete release in a few hours.

The comparison of the release speed, i.e. the time required to reach 90% of the release after 24 h, shows a faster release of [Ch][NSAID] ILs (10, 10, and 5 min for BC-[Ch][Ibu], BC-[Ch][Ket], and BC-[Ch][Nap], respectively) when compared to the original NSAIDs (60, 60, and 120 min for BC-Ibu, BC-Ket, and BC-Nap, respectively). The faster release of ILs is related to their higher solubility in PBS aqueous solutions. Similar results were obtained in studies using BC as TDDS, showing the complete release of lidocaine,²⁴ caffeine,²³ and diclofenac²² in a few minutes. Morais et al. also reported the almost complete and instantaneous release of ILs with antioxidant characteristics. The complete release of the studied [Ch][NSAID] ILs is a promising advantage to TDDS applications; it should be however remarked that the release rate can be tuned, if focusing on chronic inflammation management, by incorporating other compounds with barrier properties to reach a 24 h release requiring to change the patch only once a day.

Cytotoxicity and Anti-Inflammatory Properties of ILs and BC-ILs(*** $p < 0.001$, **** $p < 0.0001$: control vs LPS; # $p < 0.05$, ## $p < 0.01$, ### $p < 0.001$, #### $p < 0.0001$: samples vs LPS). Cytotoxicity of [Ch][NSAID] ILs and respective NSAIDs was assessed by evaluating their impact on Raw 264.7 macrophages. Figure 4 (left) shows cell viability results as a function of the NSAIDs and [Ch][NSAID] ILs concentration. EC_{50} was determined as the concentration that induces a 50% decrease in viability. Comparison of viability curves of NSAIDs and corresponding [Ch][NSAID] ILs reveals small differences, with slightly higher EC_{50} values for ILs, viz. 1.58, 2.09, 3.29, 3.30, 3.35, and 3.68 mM for Ibu, [Ch][Ibu], Ket, [Ch][Ket], Nap, and [Ch][Nap], respectively. These results show that the conversion of NSAIDs into the respective ILs does not significantly influence their cytotoxicity profile, meaning that the cholinium cations do not contribute to the cytotoxicity increase.

The cytotoxicity evaluation of BC, BC-NSAID, and BC-[Ch][NSAID] membranes was also addressed (Figure 4, right). It is shown that BC has no toxicity toward macrophages, as previously demonstrated.⁴⁸ The incorporation of NSAIDs and ILs into BC leads to similar viability profiles of the respective drugs, except with the BC-[Ch][Nap] sample that has a lower toxicity. The EC_{50} values obtained are 1.51, 2.51, 3.32, 3.03, 2.60, and >4 mM for Ibu, [Ch][Ibu], Ket, [Ch][Ket], Nap, and [Ch][Nap], respectively. Given that the viability profiles of BC-NSAIDs and BC-ILs are similar to NSAIDs and ILs, the prepared BC membranes incorporating the NSAID-based ILs can be foreseen as promising alternatives

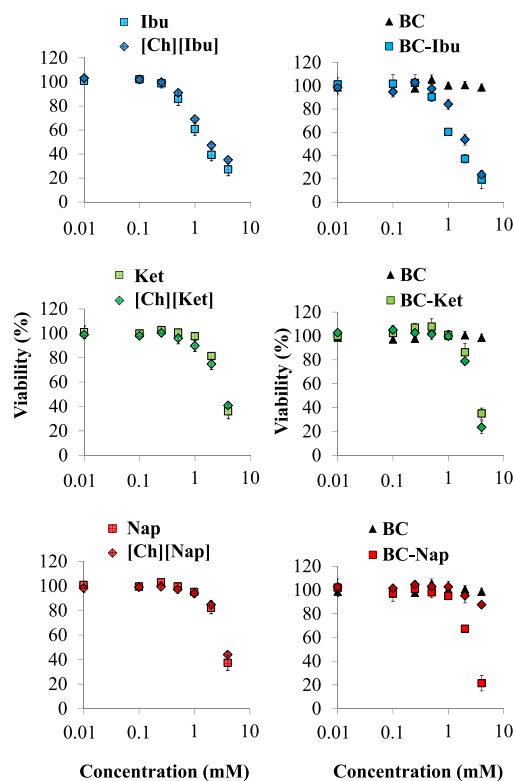


Figure 4. Viability of macrophages cells assessed as the normalized response of treated cells to untreated controls, measured by the metabolic conversion of resazurin. The data shown represents the dose–response curves of macrophages to Ibu and [Ch][Ibu] (top left); Ket and [Ch][Ket] (middle left); Nap and [Ch][Nap] (bottom left); BC, BC-Ibu, and [Ch][Ibu] (top right); BC, BC-Ket, and BC-[Ch][Ket] (middle right); BC, BC-Nap, and BC-[Ch][Nap] (bottom right).

in the development of effective patches suitable for topical applications.

The anti-inflammatory ability of ILs and BC-ILs was addressed by analyzing their effect over NO and PGE2 LPS-induced production in Raw 264.7 macrophages. The respective results are depicted in Figure 5 (top). All conditions induce a modest but significant reduction in NO production ($33.7 \pm 1.0 \mu\text{M}$ for LPS control). This behavior was expected since the main mechanism of action of the studied NSAID drugs does not rely on NO synthesis inhibition but instead on the inhibition of the cyclooxygenase-2 (COX-2) enzyme.¹ Ibu, [Ch][Ibu], BC-Ibu, and BC-[Ch][Ibu] samples result in the smaller decreases observed, displaying values of 28.9 ± 0.7 , 28.7 ± 1.0 , 29.2 ± 1.4 , and $30.9 \pm 0.9 \mu\text{M}$, respectively. On the other hand, Ket, [Ch][Ket], BC-Ket, and BC-[Ch][Ket] samples lead to the strongest decrease of NO production, with values of 18.8 ± 0.9 , 19.3 ± 0.4 , 18.3 ± 0.7 , and $19.1 \pm 0.7 \mu\text{M}$, respectively. Nap, [Ch][Nap], BC-Nap, and BC-[Ch]-[Nap] exhibit intermediary anti-inflammatory activity, namely 23.4 ± 0.8 , 24.6 ± 1.0 , 21.3 ± 0.7 , and $28.9 \pm 1.4 \mu\text{M}$, respectively. From the obtained results and compared to the original NSAIDs, it is evident that the synthesis of ionic liquids and their incorporation into BC membranes do not compromise the API capacity to inhibit LPS-induced NO production.

As mentioned above, NSAIDs inhibit the production of prostaglandins.¹ Therefore, we also investigated the impact of

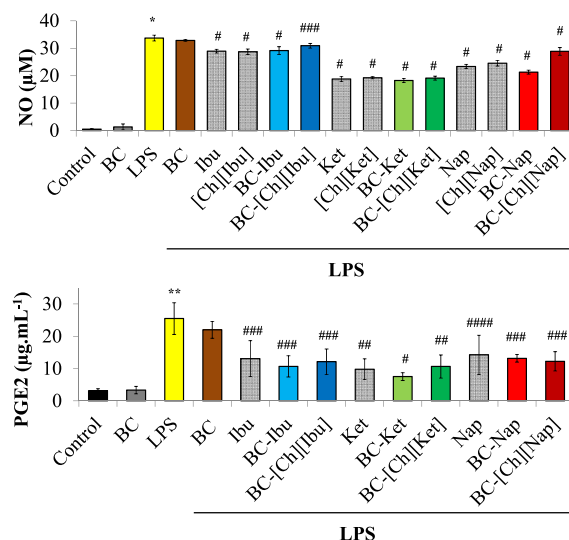


Figure 5. Evaluation of the capacity of NSAIDs, [CH][NSAID], BC-NSAIDs, and BC-[Ch][NSAID] to prevent LPS-induced NO production (top) and LPS-induced PGE2 production (bottom) in macrophages. Cells were treated with the different sample-conditioned mediums and then stimulated with LPS. (***) $p < 0.001$, (****) $p < 0.0001$: control vs LPS; (#) $p < 0.05$, (##) $p < 0.01$, (###) $p < 0.001$, (####) $p < 0.0001$: samples vs LPS).

ILs and ILs containing membranes on the LPS-induced PGE2 production (Figure 5, bottom). Similar to the assays described above, all samples exhibit a significant capacity to decrease PGE2 production ($25.5 \pm 4.9 \mu\text{g}\cdot\text{mL}^{-1}$ for LPS control). Ibu, Ket, and Nap decrease the PGE2 levels down to 13.1 ± 5.5 , 9.8 ± 3.2 , and $14.3 \pm 6.1 \mu\text{g}\cdot\text{mL}^{-1}$, respectively. As we do not observe major inhibition of PGE2 production differences between NSAIDs and their associated BC-NSAID and BC-IL membranes, it is safe to admit that there are no losses of therapeutic action. These results indirectly demonstrate the good and predictable release profile of ILs from BC membranes, as well as their noncytotoxicity, supporting their suitability for the design of topical patches with anti-inflammatory properties.

Overall, we synthesized and characterized a series of ILs composed of the cholinium cation and anions with nonsteroidal anti-inflammatory properties, namely ibuprofenate, ketoprofenate, and naproxenate. These were incorporated into bacterial nanocellulose aimed at improving topical drug delivery. The used biomaterial, bacterial cellulose, is not cytotoxic nor proinflammatory, whereas the cytotoxicity and anti-inflammatory properties of IL-incorporated BC membranes are similar to those of NSAIDs or ILs, confirming the suitability of the prepared materials for topical drug release applications.

CONCLUSIONS

In this study, ionic liquids (ILs) composed of cholinium cation and anions derived from nonsteroidal anti-inflammatory drugs (NSAID), namely ibuprofen, ketoprofen, and (S)-naproxen, were successfully synthesized and characterized. All ILs display temperatures below $100 \text{ }^\circ\text{C}$ and are thermally stable up to $181 \text{ }^\circ\text{C}$, thus allowing their use in membranes that may require sterilization achieved by temperature. The conversion of NSAIDs into cholinium-based ILs allows for an increase in their solubility in PBS aqueous solutions by 2 orders of

magnitude, which is highly beneficial to improve their bioavailability.

The prepared BC-ILs membranes are homogeneous and have thermal stability and mechanical properties suitable for topical patches applications. BC-ILs membranes have an improved rehydration capability when compared with pure BC, which is advantageous to absorb exudates, and the release of ILs is complete and fast. Biocompatibility and anti-inflammatory activity assays on ILs and BC-ILs demonstrate that there are no significant differences when compared to the original NSAIDs. These results combined with the improved bioavailability that may be afforded by the ILs higher solubility reinforce the potential application of BC-ILs membranes as safe and efficient topical delivery patches. Although no skin permeation studies have been carried out in this work, previous studies from Zhang et al.²⁵ and Morais et al.²⁶ demonstrated that imidazolium- and cholinium-based ILs have improved skin permeation rates. Therefore, further investigations should be done to assess the skin permeation rate of ILs and their impact on skin structure before applications as TDDS can be considered. Moreover, a study of the side effect of ILs on hematologic, hepatic, and cardiovascular systems could be performed as a comparison with NSAIDs side effects.

■ ASSOCIATED CONTENT

📄 Supporting Information

The Supporting Information is available free of charge on the ACS Publications website at DOI: [10.1021/acssuschemeng.9b02797](https://doi.org/10.1021/acssuschemeng.9b02797).

¹H and ¹³C liquid-state NMR of ILs, FTIR spectra of ILs and their precursors, ¹³C solid-state NMR of BC-[CH][NSAID] membranes, FTIR spectra of BC-[Ch]-[NSAID] membranes, derivatives of thermogravimetric curves of BC, BC-NSAID, and BC-[Ch][NSAID], stress/strain curves of tensile tests, parameters of Weibull model applied to BC-NSAID and BC-[Ch]-[NSAID] membranes, results on API incorporated amount in BC and on dissolution assays (PDF)

■ AUTHOR INFORMATION

Corresponding Authors

*E-mail: maragfreire@ua.pt (M.G.F.).

*E-mail: armsil@ua.pt (A.J.D.S.).

ORCID

Mukesh Sharma: 0000-0002-3438-3367

Mara G. Freire: 0000-0001-8895-0614

Carmen S. R. Freire: 0000-0002-6320-4663

Armando J. D. Silvestre: 0000-0001-5403-8416

Notes

The authors declare no competing financial interest.

■ ACKNOWLEDGMENTS

This work was developed within the scope of the European Joint Doctorate in Functional Materials Research EJD FunMat (Grant agreement ID: 641640) which funded G.C.'s Ph.D. fellowship. LCPO, CNRS UMR 5629, CICECO-Aveiro Institute of Materials FCT Ref. UID/CTM/50011/2019, and iBiMED (UID/BIM/04501/2013 and UID/BIM/04501/2019), financed by national funds through the FCT/MEC and when appropriate cofinanced by FEDER under the PT2020 Partnership Agreement, are also acknowledged.

C.S.R.F. acknowledges FCT for her research contract under Stimulus of Scientific Employment 2017 (CEECIND/00464/2017). This article was presented at the 13th International Chemical and Biological Engineering Conference (CHEMPOR 2018). The authors acknowledge the Scientific and Organizing Committees of the Conference for the opportunity to present this work.

■ REFERENCES

- (1) Wongrakpanich, S.; Wongrakpanich, A.; Melhado, K. A Comprehensive Review of Non-Steroidal Anti-Inflammatory Drug Use in The Elderly. *Aging Dis.* **2018**, *9* (1), 143–150.
- (2) Bessone, F. Non-Steroidal Anti-Inflammatory Drugs: What Is the Actual Risk of Liver Damage? *World J. Gastroenterol.* **2010**, *16* (45), 5651–5661.
- (3) Lipinski, C. A. Poor Aqueous Solubility - an Industry Wide Problem in ADME Screening. *Am. Pharm. Rev.* **2002**, *5*, 82–85.
- (4) Galico, D. A.; Holanda, B. B.; Perpétuo, G. L.; Schnitzler, E.; Treu-Filho, O.; Bannach, G. Thermal and Spectroscopic Studies on Solid Ketoprofen of Lighter Trivalent Lanthanides. *J. Therm. Anal. Calorim.* **2012**, *108* (1), 371–379.
- (5) Koç, F. E.; Şenel, M. Solubility Enhancement of Non-Steroidal Anti-Inflammatory Drugs (NSAIDs) Using Polypolypropylene Oxide Core PAMAM Dendrimers. *Int. J. Pharm.* **2013**, *451* (1–2), 18–22.
- (6) Kocbek, P.; Baumgartner, S.; Kristl, J. Preparation and Evaluation of Nanosuspensions for Enhancing the Dissolution of Poorly Soluble Drugs. *Int. J. Pharm.* **2006**, *312* (1–2), 179–186.
- (7) Rogers, R. D.; Seddon, K. R. Ionic Liquids - Solvents of the Future? *Science* **October 31, 2003**, 792–793.
- (8) Marrucho, I. M.; Branco, L. C.; Rebelo, L. P. N. Ionic Liquids in Pharmaceutical Applications. *Annu. Rev. Chem. Biomol. Eng.* **2014**, *5* (1), 527–546.
- (9) Broh-Kahn, R. H.; Sasmor, E. J. Choline Salicylate Composition and Method of Use. US Patent: 3069321, 1962.
- (10) Florindo, C.; Araújo, J. M. M.; Alves, F.; Matos, C.; Ferraz, R.; Prudêncio, C.; Noronha, J. P.; Petrovski, Z.; Branco, L.; Rebelo, L. P. N.; et al. Evaluation of Solubility and Partition Properties of Ampicillin-Based Ionic Liquids. *Int. J. Pharm.* **2013**, *456* (2), 553–559.
- (11) Shadid, M.; Gurau, G.; Shamshina, J. L.; Chuang, B. C.; Hailu, S.; Guan, E.; Chowdhury, S. K.; Wu, J. T.; Rizvi, S. A. A.; Griffin, R. J.; et al. Sulfasalazine in Ionic Liquid Form with Improved Solubility and Exposure. *MedChemComm* **2015**, *6* (10), 1837–1841.
- (12) Santos, M. M.; Raposo, L. R.; Carrera, G. V. S. M.; Costa, A.; Dionísio, M.; Baptista, P. V.; Fernandes, A. R.; Branco, L. C. Ionic Liquids and Salts from Ibuprofen as Promising Innovative Formulations of an Old Drug. *ChemMedChem* **2019**, *14* (9), 907–911.
- (13) Stolberg, V. B. *Painkillers: History, Science, and Issues*, 1st ed.; ABC-CLIO, Ed.; Greenwood: Santa Barbara, CA, 2016.
- (14) Sostres, C.; Gargallo, C. J.; Arroyo, M. T.; Lanás, A. Adverse Effects of Non-Steroidal Anti-Inflammatory Drugs (NSAIDs, Aspirin and Coxibs) on Upper Gastrointestinal Tract. *Best Pract. Res. Clin. Gastroenterol.* **2010**, *24* (2), 121–132.
- (15) Rogers, R. D.; Seddon, K. R. Ionic Liquids - Solvents of the Future? *Science* **2003**, 792–793.
- (16) Kandavilli, S.; Nair, V.; Panchagnula, R. Polymers in Transdermal Drug Delivery Systems. *Pharm. Technol.* **2002**, *1*, 62–80.
- (17) Valenta, C.; Auner, B. G. The Use of Polymers for Dermal and Transdermal Delivery. *Eur. J. Pharm. Biopharm.* **2004**, *58* (2), 279–289.
- (18) Tombs, E. L.; Nikolaou, V.; Nurumbetov, G.; Haddleton, D. M. Transdermal Delivery of Ibuprofen Utilizing a Novel Solvent-Free Pressure-Sensitive Adhesive (PSA): TEPI® Technology. *J. Pharm. Innov.* **2018**, *13* (1), 48–57.
- (19) Chawla, P. R.; Bajaj, I. B.; Survase, S. a.; Singhal, R. S. Microbial Cellulose: Fermentative Production and Applications. *Food Technol. Biotechnol.* **2009**, *47* (2), 107–124.

- (20) Bodhibukkana, C.; Srichana, T.; Kaewnopparat, S.; Tangthong, N. *J. Controlled Release* **2006**, *113*, 43–56.
- (21) Wei, B.; Yang, G.; Hong, F. Preparation and Evaluation of a Kind of Bacterial Cellulose Dry Films with Antibacterial Properties. *Carbohydr. Polym.* **2011**, *84* (1), 533–538.
- (22) Silva, N. H. C. S.; Rodrigues, A. F.; Almeida, I. F.; Costa, P. C.; Rosado, C.; Neto, C. P.; Silvestre, A. J. D.; Freire, C. S. R. Bacterial Cellulose Membranes as Transdermal Delivery Systems for Diclofenac: In Vitro Dissolution and Permeation Studies. *Carbohydr. Polym.* **2014**, *106* (1), 264–269.
- (23) Silva, N. H. C. S.; Drumond, I.; Almeida, I. F.; Costa, P.; Rosado, C. F.; Neto, C. P.; Freire, C. S. R.; Silvestre, A. J. D. Topical Caffeine Delivery Using Biocellulose Membranes: A Potential Innovative System for Cellulite Treatment. *Cellulose* **2014**, *21* (1), 665–674.
- (24) Trovatti, E.; Freire, C. S. R.; Pinto, P. C.; Almeida, I. F.; Costa, P.; Silvestre, A. J. D.; Neto, C. P.; Rosado, C. Bacterial Cellulose Membranes Applied in Topical and Transdermal Delivery of Lidocaine Hydrochloride and Ibuprofen: In Vitro Diffusion Studies. *Int. J. Pharm.* **2012**, *435* (1), 83–87.
- (25) Zhang, D.; Wang, H. J.; Cui, X. M.; Wang, C. X. Evaluations of Imidazolium Ionic Liquids as Novel Skin Permeation Enhancers for Drug Transdermal Delivery. *Pharm. Dev. Technol.* **2017**, *22* (4), 511–520.
- (26) Morais, E. S.; Silva, N. H. C. S.; Sintra, T. E.; Santos, A. O.; Neves, B. M.; Isabel, F.; Costa, P. C.; Correia-Sa, I.; Ventura, S. P. M.; Silvestre, A. J. D.; et al. Anti-Inflammatory and Antioxidant Nanostructured Cellulose Membranes Loaded with Phenolic-Based Ionic Liquids for Cutaneous Application. *Carbohydr. Polym.* **2019**, *206*, 187–197.
- (27) Sintra, T. E.; Luís, A.; Rocha, S. N.; Ferreira, A. I. M. C. L.; Gonçalves, F.; Santos, L. M. N. B. F.; Neves, B. M.; Freire, M. G.; Ventura, S. P. M.; Coutinho, J. A. P. Enhancing the Antioxidant Characteristics of Phenolic Acids by Their Conversion into Cholinium Salts. *ACS Sustainable Chem. Eng.* **2015**, *3* (10), 2558–2565.
- (28) Trovatti, E.; Serafim, L. S.; Freire, C. S. R.; Silvestre, A. J. D.; Neto, C. P. Gluconacetobacter Sacchari: An Efficient Bacterial Cellulose Cell-Factory. *Carbohydr. Polym.* **2011**, *86* (3), 1417–1420.
- (29) Hestrin, S.; Schramm, M. Synthesis of Cellulose by Acetobacter Xylinum. Preparation of Freeze-Dried Cells Capable of Polymerizing Glucose to Cellulose. *Biochem. J.* **1954**, *58* (2), 345–352.
- (30) Paroha, S.; Dubey, R. D. Physicochemical Interaction of Naproxen with Aluminium Hydroxide and Its Effect on Dissolution. *Farmacia* **2013**, *61*, 103–115.
- (31) Isik, M.; Gracia, R.; Kollnus, L. C.; Tome, L. C.; Marrucho, I. M.; Mecerreyes, D. Cholinium Lactate Methacrylate: Ionic Liquid Monomer for Cellulose Composites and Biocompatible Ion Gels. *Macromol. Symp.* **2014**, *342* (1), 21–24.
- (32) Gadilohar, B. L.; Shankarling, G. S. Choline Based Ionic Liquids and Their Applications in Organic Transformation. *J. Mol. Liq.* **2017**, *227*, 234–261.
- (33) Petkovic, M.; Ferguson, J. L.; Gunaratne, H. Q. N.; Ferreira, R.; Leitão, M. C.; Seddon, K. R.; Rebelo, L. P. N.; Pereira, C. S. Novel Biocompatible Cholinium-Based Ionic Liquids - Toxicity and Biodegradability. *Green Chem.* **2010**, *12* (4), 643–649.
- (34) Seddon, K. R. Ionic Liquids for Clean Technology. *J. Chem. Technol. Biotechnol.* **1997**, *68* (4), 351–356.
- (35) Saïdi, L.; Vilela, C.; Oliveira, H.; Silvestre, A. J. D.; Freire, C. S. R. Poly(N-Methacryloyl Glycine)/Nanocellulose Composites as pH-Sensitive Systems for Controlled Release of Diclofenac. *Carbohydr. Polym.* **2017**, *169*, 357–365.
- (36) Tita, B.; Fuliás, A.; Tita, D. Kinetic Study of Ibuprofen under Isothermal Conditions. *Rev. Chim. (Bucharest, Rom.)* **2010**, *61* (11), 1037–1041.
- (37) Tița, D.; Fuliás, A.; Tița, B. Thermal Stability of Ketoprofen: Part 2. Kinetic Study of the Active Substance under Isothermal Conditions. *J. Therm. Anal. Calorim.* **2013**, *111* (3), 1979–1985.
- (38) Sovizi, M. R. Thermal Behavior of Drugs: Investigation on Decomposition Kinetic of Naproxen and Celecoxib. *J. Therm. Anal. Calorim.* **2010**, *102* (1), 285–289.
- (39) Dudognon, E.; Danède, F.; Descamps, M.; Correia, N. T. Evidence for a New Crystalline Phase of Racemic Ibuprofen. *Pharm. Res.* **2008**, *25* (12), 2853–2858.
- (40) Sailaja, U.; Shahin Thayyil, M.; Krishna Kumar, N. S.; Govindaraj, G. Molecular Dynamics in Liquid and Glassy States of Non-Steroidal Anti-Inflammatory Drug: Ketoprofen. *Eur. J. Pharm. Sci.* **2013**, *49* (2), 333–340.
- (41) Alleso, M.; Chieng, N.; Rehder, S.; Rantanen, J.; Rades, T.; Aaltonen, J. Enhanced Dissolution Rate and Synchronized Release of Drugs in Binary Systems through Formulation: Amorphous Naproxen-Cimetidine Mixtures Prepared by Mechanical Activation. *J. Controlled Release* **2009**, *136* (1), 45–53.
- (42) Silva, N. H. C. S.; Rodrigues, A. F.; Almeida, I. F.; Costa, P. C.; Rosado, C.; Neto, C. P.; Silvestre, A. J. D.; Freire, C. S. R. Bacterial Cellulose Membranes as Transdermal Delivery Systems for Diclofenac: In Vitro Dissolution and Permeation Studies. *Carbohydr. Polym.* **2014**, *106*, 264–269.
- (43) Trovatti, E.; Silva, N. H. C. S.; Duarte, I. F.; Rosado, C. F.; Almeida, I. F.; Costa, P.; Freire, C. S. R.; Silvestre, A. J. D.; Neto, C. P. Biocellulose Membranes as Supports for Dermal Release of Lidocaine. *Biomacromolecules* **2011**, *12* (11), 4162–4168.
- (44) Donnelly, R. F.; McCrudden, M. T. C.; Alkilani, A. Z.; Larrañeta, E.; McAlister, E.; Courtenay, A. J.; Kearney, M. C.; Raj Singh, T. R.; McCarthy, H. O.; Kett, V. L. Hydrogel-Forming Microneedles Prepared from “Super Swelling” Polymers Combined with Lyophilised Wafers for Transdermal Drug Delivery. *PLoS One* **2014**, *9* (10), e111547.
- (45) Adeyeye, C. M.; Price, J. C. Development and Evaluation of Sustained-Release Ibuprofen–Wax Microspheres. II. In Vitro Dissolution Studies. *Pharm. Res.* **1994**, *11*, 575–579.
- (46) Mazieres, B. Topical Ketoprofen Patch. *Drugs R&D* **2005**, *6* (6), 337–344.
- (47) Khatun, M.; Islam, S. A.; Akter, P.; Quadir, M. A.; Reza, M. S. Controlled Release of Naproxen Sodium from Eudragit RS 100 Transdermal Film. *Dhaka Univ. Dhaka Univ. J. Pharm. Sci.* **2004**, DOI: 10.3329/dujps.v3i1.175.
- (48) Wang, B.; Lv, X.; Chen, S.; Li, Z.; Sun, X.; Feng, C.; Wang, H.; Xu, Y. In Vitro Biodegradability of Bacterial Cellulose by Cellulase in Simulated Body Fluid and Compatibility in Vivo. *Cellulose* **2016**, *23* (5), 3187–3198.